

# Barnes–Evans relations for late–type giants and dwarfs

K. Beuermann<sup>1</sup>, I. Baraffe<sup>2</sup>, and P. Hauschildt<sup>3</sup>

<sup>1</sup> Universitäts-Sternwarte, Geismarlandstrasse 11, D-37083 Göttingen, Germany

<sup>2</sup> C.R.A.L. (UMR 5574 CNRS), Ecole Normale Supérieure de Lyon, F-69364 Lyon Cedex 0.7, France

<sup>3</sup> Department of Physics and Astronomy and Center for Simulational Physics, University of Georgia, Athens, GA 30602-2451, USA

Received 19 March 1999 / Accepted 18 June 1999

**Abstract.** The visual surface brightness of K/M giants and dwarfs with near-solar metallicity differ slightly in agreement with the gravity effects predicted by recent theoretical models. We show that M-dwarfs display also a metallicity dependence of the surface brightness in the infrared *K*-band in agreement with theory. Based on these results, we present improved Barnes-Evans type relations and estimate the radii of 60 single or presumed M and K-dwarfs.

**Key words:** stars: abundances – stars: atmospheres – stars: late-type

## 1. Introduction

Barnes & Evans (1976) showed that a tight relation exists between the visual surface brightness and the colour of giants. Such a relation allows to determine the angular diameter and, if the distance is known, the radius of a star from photometric data alone (Lacy 1977, Dumm & Schild 1998). Lacy assumed that the Barnes-Evans relation derived for giants holds also for dwarfs, but this has never been actually proved.

For giants, additional measurements of the angular diameters have become available in recent years (Dumm & Schild 1998, Dyck et al. 1998, and references therein). Angular diameters of dwarfs can so far not be measured directly, but can be derived from bolometric fluxes and temperatures or, more accurately, from flux scaling of model atmospheres to the low-resolution optical/IR overall spectral energy distributions. Leggett et al. (1996, hereafter L96) have applied this method to 16 M-dwarfs using the advanced *NextGen* M-dwarf model atmospheres of Hauschildt et al. (1999). There is excellent agreement between the L96 radii and those predicted by recent stellar models (Baraffe et al. 1998, hereafter BCAH98; see the comparisons made in L96 and in Beuermann et al. 1998, henceforth Paper I). This convergence of theory and observation is generally regarded as a breakthrough and an important step towards a temperature and radius scale of stars on the lower main sequence, although there is still some concern about the remaining differences (e.g. Clemens et al. 1998).

In this paper, we use the results of L96 to derive the surface brightness of M-dwarfs. We then show that the visual surface brightness vs. Cousins  $V - I_c$  relationships for M-dwarfs differs from that of M-giants in a colour-dependent way and find a close agreement between observationally determined and theoretically predicted gravity dependencies (BCAH98, Alibert et al. 1999, Hauschildt et al. in preparation). We, furthermore, show that M-dwarfs display a metallicity dependence of the surface brightness in the infrared *K*-band which also agrees with that predicted. The good agreement between theory and observation increases our confidence in the derived Barnes-Evans relations and the implied radius scale of M-dwarfs.

## 2. The Barnes-Evans relations for giants and dwarfs

Barnes & Evans (1976) defined the surface brightness as<sup>1</sup>

$$F_\lambda = -0.1m_\lambda - 0.5 \log \phi + 4.2211 \quad (1)$$

where  $m_\lambda$  is the apparent magnitude at wavelength  $\lambda$  and  $\phi$  is the angular diameter of the star in mas. With the absolute magnitude  $M_\lambda$  and the radius  $R$  of the star, Eq. (1) can be cast into the form (e.g. Bailey 1981)

$$S_\lambda = M_\lambda + 5 \log(R/R_\odot) = -10 F_\lambda + 42.368. \quad (2)$$

Fig. 1 compares the visual surface brightness vs. Cousins  $V - I_c$  relationships for late-type giants and dwarfs. The giant sample includes 28 stars from Dumm & Schild (1998) with spectral types M0 to M7 ( $1.65 < V - I_c < 4.30$ ) and nine non-variable K-giants from Dyck et al. (1998). Most of the stars are of luminosity class III with a few of class II. The  $V$  magnitudes and Cousins  $V - I_c$  values were taken from the on-line version of the HIPPARCOS catalogue (entries H5 and H40), the angular diameters are from Dumm & Schild (1998) and Dyck et al. (1998, and private communication). Most of the giants in the sample are located within the local bubble where the density of atomic hydrogen is low (Diamond et al. 1995, Thomas & Beuermann 1998). Inside the bubble, reddening is usually

<sup>1</sup> The numerical constant in Eq. (1), 4.2211, equals  $1 + 0.1 M_{\text{bol},\odot} + 0.25 \log(4 f_\odot/\sigma)$ , where  $M_{\text{bol},\odot} = 4.75$  is the bolometric magnitude of the Sun,  $f_\odot = 1.368 \cdot 10^6 \text{ erg cm}^{-2} \text{ s}^{-1}$  is the solar constant, and  $\sigma$  is the Stefan-Boltzmann constant.

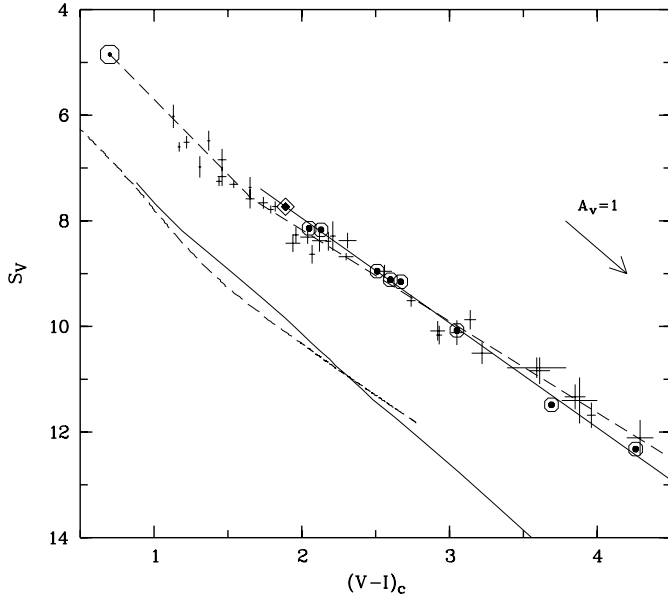


**Fig. 1.** Visual surface brightness  $S_V$  vs. Cousins  $V - I_c$  for dwarfs and giants. Dwarf data are for eight YD field stars from L96 ( $\odot$ ), the mean of the two components of the eclipsing binary YY Gem ( $\diamond$ ), and the Sun ( $\circ$ ). Giant data are for 28 M-stars and 9 K-stars (+). Dashed and solid lines represent the fits of Eqs. (3) and (5). Error bars are included for the giant data. For the dwarfs, the error bars equal the size of the symbols. For illustrative purposes, the reddening path for  $A_v = 1$  is indicated on the right. Also shown are the theoretical curves for dwarfs (solid curve) and for giants (dashed curve), displaced downward by two units for clarity (see text for the differences in slope).

small and the standard reddening corrections based on distance and latitude (e.g. Fouqué & Gieren 1997) are of limited use. We opted not to apply reddening corrections, therefore. There may be a problem, however, with circumstellar absorption in some of the stars of latest spectral type (see e.g. the comments in Dumm & Schild 1998). We excluded one star from the giant sample,  $\tau^4$  Ser, which leaves us with 27 stars. For illustrative purposes, we show in Fig. 1 the reddening path for a standard interstellar absorption of  $A_v = 1$  with  $A_v = 2.41 E_{V-I}$  (Schlegel et al. 1998), but expect that none of the giants shows this much absorption. Since most of the M-giants are more or less variable, errors due to the non-simultaneity of the brightness and angular diameter measurements probably dominate the observed scatter in  $S_V$ . The error bars are, therefore, determined by quadratically adding the variability amplitude (1/2 of the difference in fields H50 and H49 in the HIPPARCOS catalogue), a minimum uncertainty in the  $V$ -magnitude, taken to be 0.02 mag, and the error in  $5 \log \phi$ . The standard error in  $V - I_c$  is taken from entry H41 of the HIPPARCOS catalogue. A linear fit for the 27 M-giants yields

$$S_{V,\text{giants}} = 4.71(\pm 0.14) + 1.74(\pm 0.05)(V - I_c) \quad (3)$$

which agrees with the fit of Dumm & Schild (1998, their Eq. [5]) within the  $1\sigma$  errors. The scatter in the giant data is a source of concern for the dwarf-giant comparison. We can not exclude that this comparison is affected by remaining systematic errors

in the giant data, like selection effects, variability, and circumstellar reddening, which are difficult to estimate. It is comforting, though, that Eq. (3) is consistent with the red section of the original relation of Barnes & Evans (1976) which was given as a function of Johnson  $V - R_J$ . Our result is also consistent with the  $S_V$  vs.  $V - K$  relations for Cepheids, field giants and field supergiants discussed by Fouqué & Gieren (1997). Using SIMBAD  $K$ -magnitudes for 16 of our M-giants, we obtain

$$S_{V,\text{giants}} = 3.82(\pm 0.10) + 1.00(\pm 0.05)(V - K) \quad (4)$$

which is valid for  $3.5 < V - K < 7$  and agrees with the red part of the Fouqué & Gieren relation (see their Fig. 3).

For K-giants ( $V - I_c < 1.65$ ), the relation in Fig. 1 steepens. This change of slope was already noted by Barnes & Evans (1976) and Barnes et al. (1977) who also showed that there is no difference in the surface brightness of giants and dwarfs for stars of spectral types B–G and found the Sun to fall on the giant relation. Tying the fit to the Sun at  $V - I_c = 0.70$ ,  $S_V = 4.85$ , we obtain  $S_V = 2.86 + 2.84(V - I_c)$  for  $V - I_c < 1.65$ . All Barnes-Evans type relations for giants suggest that the slope of the relation changes near the transition from K to M-stars. In summary, the results for giants presented here coincide closely with those of other authors.

The dwarf data in Fig. 1 include eight young disk (YD) M-dwarfs from L96 and the YD eclipsing binary YY Gem of spectral type M1+M1. The angular diameters and effective temperatures  $T_{\text{eff}}$  were derived by L96 from flux fitting of the Hauschildt et al. (1999) *NextGen* model atmospheres to the observed low-resolution optical/IR spectra. L96 consider the angular diameters obtained by this approach to be less fallible to errors in  $T_{\text{eff}}$  than those derived from the observational bolometric magnitude and  $T_{\text{eff}}$ . They quote an error of 2% in the derived angular diameters. An additional uncertainty in the radii may, however, arise from errors in the flux fitting procedure. The integrated luminosities of the best-fit models quoted by L96 tend to fall below the observed luminosity, i.e.  $M_{\text{bol}}' = -2.5 \log(4\pi R^2 \sigma T_{\text{eff}}^4 / L_{\odot}) + M_{\text{bol},\odot} > M_{\text{bol}}$ , with  $R$  and  $T_{\text{eff}}$  as derived by L96 and the  $>$  sign implying “fainter than”. For the eight L96 YD stars, the flux deficiency averages  $\sim 0.15$  mag relative to  $M_{\text{bol}} = M_V + BC_V$ , with  $BC_V$  the visual bolometric correction as given by L96 (their Table 6), and  $\sim 0.10$  mag relative to  $M_{\text{bol}} = M_K + BC_K$ , with the bolometric correction in the  $K$ -band from Tinney et al. (1993). While it is well known that bolometric magnitudes are uncertain by as much as 0.10 mag (see e.g. the discussion in L96 and their Fig. 7), the amount of the flux deficiency suggests that either the temperatures of L96 are low by  $\sim 3\%$ , their radii by  $\sim 6\%$ , or both by correspondingly smaller percentages. Accepting the radii implies that the temperatures of the eight YD stars are on the average too low by 90 K which is well within the temperature errors, whereas accepting the temperatures leads to angular diameters (not radii which include the parallax errors) outside the quoted range. We assume, therefore, that the radii are basically correct and proceed to use them for calibrating our Barnes-Evans relation for dwarfs. The possible  $\sim 6\%$  systematic uncertainty in the angular diameters corresponds to an

uncertainty of 0.13 in  $S_V$  which may affect the absolute level of  $S_V$  but probably not the slope of the  $S_V(V - I_c)$  relation. The L96 YD dwarfs are well observed with an error in  $V - I_c$  less than  $\sim 0.05$ . Both error bars, in  $S_V$  and  $V - I_c$ , are of the size of the dwarf data points in Fig. 1.

Finally, the mean angular diameter of the two components of YY Gem was calculated from their observed radii (Leung & Schneider 1978) and the HIPPARCOS parallax of 63.2mas. Note that there is no systematic difference between the surface brightness of YY Gem and that established for YD dwarfs by the radius scale of L96.

A linear fit to the data in Fig. 1, i.e. the eight YD dwarfs from L96 and to YY Gem, yields

$$S_{V,YD \text{ dwarfs}} = 3.99(\pm 0.13) + 1.98(\pm 0.05)(V - I_c) \quad (5)$$

which is valid for  $V - I_c > 1.65$ . Comparison of Eqs. (3) and (5) shows that there is a difference in slope of  $0.24 \pm 0.07$  which is significant at the  $3.5\sigma$  level. The absolute levels of the giant and dwarf fits suggest that the visual surface brightness of early M-dwarfs is slightly higher than that of M-giants, reaching a separation of  $0.30 \pm 0.09$  mag at spectral type K7/M0 ( $V - I_c = 1.65$ ). Since there are no equally reliable radii for K-dwarfs, the extension to  $V - I_c < 1.65$  is not covered. There is no difference in the surface brightness of giants and dwarfs for stars of spectral types B–G (Barnes & Evans 1976, Barnes et al. 1977), however, which suggests that the observational dwarf relation in Fig. 1 should connect to the Sun, that the dwarf/giant difference reaches a maximum for late K and early M stars, and that the break in the  $S_V(V - I_c)$  relation near  $V - I_c = 1.65$  is less pronounced for dwarfs than for giants. This observation suggests the presence of gravity effects in the surface brightness vs. colour relation.

Fig. 1 also compares the observational results with the predictions of recent theoretical work for late-type giants (Alibert et al. 1999, Hauschildt et al. in preparation) and late-type dwarfs (BCAH98), both of solar composition. The  $S_V(V - I_c)$  relationship predicted for solar-metallicity ZAMS dwarfs with masses from  $1.2 M_\odot$  down to  $0.075 M_\odot$  is shown as solid curve (for clarity shifted downward by two units). The corresponding relationship for giants (dashed curve) is represented by the post main sequence evolutionary track of a  $12 M_\odot$  star, evolved until central carbon ignition. Details of the calculations can be found in the recent work of Alibert et al. (1999) on Cepheids which shows a generally good agreement between models and recent observations in period–magnitude and period–radius diagrams. We note that tracks from  $4 M_\odot$  to  $12 M_\odot$  are very similar in the  $S_V$  vs.  $V - I_c$  diagram. This is in agreement with the results of Fouqué & Gieren (1997), who find that giant and supergiant surface brightness relations are indistinguishable. Therefore, the  $12 M_\odot$  track shown in Fig. 1 is representative of the  $S_V(V - I_c)$  relationship expected for giant and supergiants, with gravities  $\log g = 0\text{--}3$  and effective temperatures  $T_{\text{eff}} = 3500\text{--}7000$  K.

The differences in the slopes and normalizations of Eqs. (3) and (5) as well as the different strengths of the break for giants and dwarfs at the K/M transition ( $V - I_c = 1.65$ ) agree quantitatively with those predicted by the stellar models. For the range

in  $V - I_c$  covered here, the theoretical  $S_V(V - I_c)$  relationships for giants and dwarfs reach a maximum separation of  $\Delta S_V = 0.35$  mag at  $V - I_c = 1.65$ , very similar to the observed difference of 0.30 mag from Eqs. (3) and (5). Since the giant  $S_V$  is based on observed angular diameters and we consider the theoretical prediction of the difference in  $S_V$  reliable, the dwarf  $S_V$  and, hence, the dwarf radius scale can not be seriously in error either.

For an early M-star of given  $M_V$ , a difference in  $S_V$  for giants and dwarfs of  $\Delta S_V = 0.30$  mag corresponds to a difference in radius of 15%. I.e., if the giant calibration were used for dwarfs, the derived radii at  $V - I_c = 1.65$  (spectral type K7) would be 15% too large.

For later spectral types, the difference becomes smaller and even reverses sign near  $V - I_c = 2.9$ , or spectral type M4.5. Models for giants of still later spectral type ( $T_{\text{eff}} < 3500$  K) are not yet available and the comparison between observation and theory is restricted to spectral types earlier than M4. A quantitative comparison of the absolute values of  $S_V$  is limited by the fact that the theoretical  $V$ -magnitudes of M-stars calculated with the most recent models are still somewhat too bright and the colours involving  $V$  too blue (see also Fig. 2b which shows the corresponding effect in the colour  $V - K$ ). This remaining error in the theory is suspected to be due to uncertainties in the molecular absorption coefficients for solar-metallicity stars in the visual passband (BCAH98). It causes the slopes of the  $S_V(V - I_c)$  relations of both M-giants and M-dwarfs at  $V - I_c \gtrsim 1.6$  to be too steep, but should, to a first approximation, not affect the ordinate *difference* of the two curves which measures the gravity effect. Since the error in the theoretical  $V$ -magnitudes of late-type stars with near-solar metallicity reaches about 0.6 mag (see Fig. 3b) the corrected theoretical crossover between the  $S_V(V - I_c)$  relations of giants and dwarfs occurs at  $V - I_c \simeq 2.9$  rather than  $V - I_c = 2.3$ , which is just as observed.

While our results show that a slight gravity effect in the  $S_V(V - I_c)$  relation is present, the calibrations of Eqs. (3) and (5) are never further apart than 0.3 mag. This *approximate* equality is the observational and theoretical basis for Lacy's (1977) approach to determine the radii of late-type dwarfs from the Barnes-Evans relation for giants.

### 3. Metallicity dependence of $S_K$ for M-dwarfs

In addition to gravity, metallicity affects the surface brightness at a given colour. Given the steepness of the  $S_V(V - I_c)$  relation, however, the dependence of the observational data on metallicity is easily obliterated by errors in  $V - I_c$ . It is more readily detectable in the infrared  $K$ -band because  $S_K$  is a much shallower function of colour.

The models suggest that the metallicity dependence appears only at temperatures sufficiently low that molecules are present. For giants and supergiants with  $T_{\text{eff}} > 3500$  K, corresponding to  $V - I_c < 2$ , the models of Alibert et al. (1999) indicate a very small dependence on metallicity. At these higher temperatures,  $S_V$  and  $S_K$  at given  $V - I_c$  or  $I_c - K$  vary by less than 0.05 mag for metallicities between  $[M/H] = 0$  and  $-0.7$ . For dwarfs, the

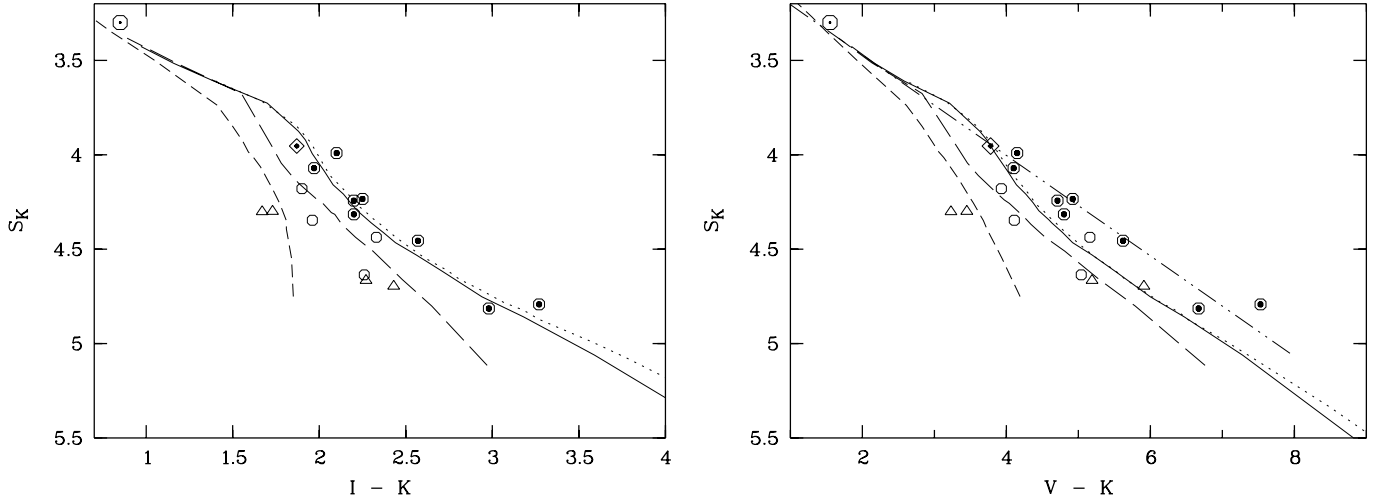


**Fig. 2.** Barnes-Evans type relations  $S_K$  vs.  $I_c - K$  and  $V - K$  with the  $K$ -band magnitudes being on the CIT system. The data points indicate the L96 dwarfs: YD ( $\odot$  and  $\diamond$ ), OD ( $\circ$ ), and H ( $\triangle$ ). The curves indicate the theoretical models of BCAH98 for ZAMS stars with solar metallicity  $[M/H]=0$  (solid curve), for solar-metallicity stars aged 0.1 Gyr (dotted), and for stars aged 10 Gyrs with metallicities  $[M/H] = -0.5$  (long dashes) and  $[M/H] = -1.5$  (short dashes). The dot-dashed line in the right-hand panel (b) represents the fit of Eq. (6) to the YD data.

main metallicity effects appear for  $V - I_c \gtrsim 1.8$  (BCAH98), a regime which is largely unexplored for giants.

In Fig. 2ab, we compare the observed values of  $S_K$  vs.  $I_c - K$  and  $V - K$  for the 16 dwarfs of L96 supplemented by YY Gem and the Sun with the predictions of the models of BCAH98 for main-sequence dwarfs. The theoretical curves refer to ZAMS models with solar metallicity  $[M/H] = 0$  (solid curves) and to models for stars aged 10 Gyr with metallicities  $-0.5$  (long dashes) and  $-1.5$  (short dashes). Pre-main-sequence stars of solar composition aged  $10^8$  years (dotted curves) and ZAMS stars of the same colour agree closely in surface brightness, except for very late spectral types where the  $10^8$ -yrs isochrone is sufficiently far from the ZAMS for gravity effects to become apparent. For these pre-main-sequence stars  $S_K$  is enhanced and differs from ZAMS dwarfs in the same way as is evident for late-type giants in Fig. 1.

Fig. 2a demonstrates that the main-sequence models reproduce the observed level of  $S_K$ , its variation with  $I_c - K$ , and the spread with metallicity exceedingly well. The agreement between observation and theory is less good for  $S_K$  vs.  $V - K$  in Fig. 2b because, as noted above, the theoretical colours of solar-metallicity M-stars with  $V - K \gtrsim 4$  which involve  $V$  are too blue (by about half a magnitude). This uncertainty in  $V$  is much smaller for dwarfs of lower metallicity. For the purpose of determining radii via Eq. (2), we provide the surface brightness values of the BCAH98 models in Table 1, except for  $S_K(V - K)$  of stars with solar metallicity for which we approximate the data for the eight L96 YD dwarfs, YY Gem, and the Sun by the *linear* relation

$$S_{K,\text{YD dwarfs}} = 2.95(\pm 0.08) + 0.266(\pm 0.017)(V - K). \quad (6)$$

The limited statistics of the L96 sample does not warrant a higher-order fit, but the real  $S_K(V - K)$  relation for solar-metallicity stars will certainly show some structure caused by molecule formation and the onset of convection in the optically

**Table 1.** Model values of the surface brightness  $S_K$  in the K-band as functions of  $I_c - K$  and  $V - K$  for ZAMS stars with solar metallicity and stars aged 10 Gyr with 1/3 solar metallicity (from BCAH98). The  $K$ -band magnitudes are on the CIT system.

Mass $M_\odot$	ZAMS, $[M/H] = 0$			10 Gyrs, $[M/H] = -0.5$			
	$M_K$	$I_c - K$	$S_K$	$M_K$	$I_c - K$	$V - K$	$S_K$
1.00	3.49	0.97	3.43				
0.80	3.98	1.30	3.57	3.62	0.89	1.67	3.38
0.70	4.49	1.65	3.70	4.26	1.17	2.13	3.51
0.60	5.08	1.92	3.89	4.82	1.55	2.83	3.68
0.50	5.74	2.06	4.11	5.56	1.73	3.32	3.96
0.45	6.04	2.11	4.16	5.92	1.78	3.46	4.04
0.40	6.32	2.16	4.21	6.25	1.84	3.61	4.11
0.35	6.59	2.20	4.26	6.55	1.88	3.72	4.15
0.30	6.88	2.23	4.29	6.83	1.92	3.81	4.18
0.25	7.24	2.29	4.33	7.20	1.99	3.97	4.24
0.20	7.71	2.37	4.41	7.67	2.09	4.21	4.32
0.175	7.99	2.44	4.45	7.96	2.13	4.34	4.37
0.150	8.33	2.55	4.53	8.30	2.21	4.54	4.44
0.130	8.66	2.70	4.61	8.63	2.31	4.81	4.51
0.110	9.09	2.95	4.74	9.10	2.48	5.29	4.66
0.100	9.39	3.17	4.85	9.44	2.65	5.79	4.80
0.090	9.81	3.58	5.06	10.00	2.97	6.76	5.12
0.080	10.57	4.40	5.54	11.50	3.92	9.48	6.27

thin layers of the atmosphere, as does the  $S_K(I_c - K)$  relation at  $I_c - K \simeq 1.9$ .

#### 4. The $R(M_K)$ relation of $[M/H] \simeq 0$ ZAMS dwarfs

For stars of given age and metallicity, theory provides the radius as a function of absolute magnitude, e.g.  $M_K$ . In the present context this follows from the fact that the models yield  $V - K$  as a function of  $M_K$  which transforms Eq. (6) into  $S_K(M_K)$  and Eq. (2) into  $R(M_K)$ .

Fig. 3a shows the observed radii of YY Gem (mean component) and the eight YD, four old disk (OD), and four halo (H) M-dwarfs of L96 along with the BCAH98 model radii for solar-composition ZAMS stars (solid curve, see also Fig. 1 of Paper I). There is no obvious difference between the radii of YD and OD stars in this rather restricted sample. The two faint H stars show the expected smaller radii. This is consistent with the small metallicity dependence of the  $R(M_K)$  BCAH98 models which can approximately be expressed by  $\Delta \log R \simeq -0.03$  per 1 dex reduction of  $[M/H]$  relative to solar (BCAH98). On the average, the L96 radii of the YD/OD stars exceed the  $[M/H] = 0$  ZAMS model radii by 2% (Paper I) which is within the systematic uncertainties of the L96 radii. These model radii (solid curve) can be represented reasonably well by a third-order polynomial in  $M_K$  which we adjust slightly, by  $\Delta \log R = +0.009$ , to nominally fit the L96 radii (dot-dashed curve in Fig. 3a)

$$\log \frac{R}{R_\odot} = -0.022 + 0.1294 M_K - 0.04464 M_K^2 + 0.002237 M_K^3. \quad (7)$$

We accept Eq. (7) as representative of ZAMS stars with near-solar or slightly reduced metallicities (kinematic classes YD and OD). Note that radii for stars fainter than  $M_K \simeq 10$  are still uncertain because dust formation is not accounted for in the BCAH98 models

Stellar radii may be estimated either from a Barnes-Evans type relation as Eq. (6) together with Eq. (2) or directly from the  $R(M_K)$  relation in Eq. (7). The former depends weakly on gravity but distinctly on metallicity, while the latter depends weakly on metallicity and strongly on gravity and, therefore, requires knowledge of the evolutionary status.

The different metallicity dependencies of the two approaches arise because reference is taken to a colour in one case and directly to the absolute magnitude in the other. The difference in the approaches becomes more obvious when combining Eqs. (2), (6), and (7) to yield the colour-magnitude relation  $V - K$  vs.  $M_K$  for ZAMS stars of near-solar metallicity

$$V - K = -11.50 + 6.215 M_K - 0.8423 M_K^2 + 0.04221 M_K^3. \quad (8)$$

(Fig. 3b, dot-dashed curve). Eq. (8) closely fits the L96 YD stars (encircled dots) which is as expected because Eqs. (6) and (7) fit these stars, too. Although Eq. (7) is approximately valid also for OD stars with slightly reduced metallicity, Eq. (6) and Eq. (8) are not. At the *same*  $M_K$ , stars of lower metallicity (open points, triangles in Fig. 3b) are bluer. They have nearly unchanged  $S_K$  and radii, however, because the metallicity dependence of the colour in Fig. 3b and the metallicity dependence of  $S_K(V - K)$  in Fig. 2b compensate approximately. This implies that application of the Barnes-Evans relations in Fig. 2 requires knowledge of the metallicity of the respective stars.

## 5. Radii of main-sequence M-dwarfs

In this section, we test our results on the 12 YD/OD stars of L96 which serve as calibrators and then apply them to a sample of

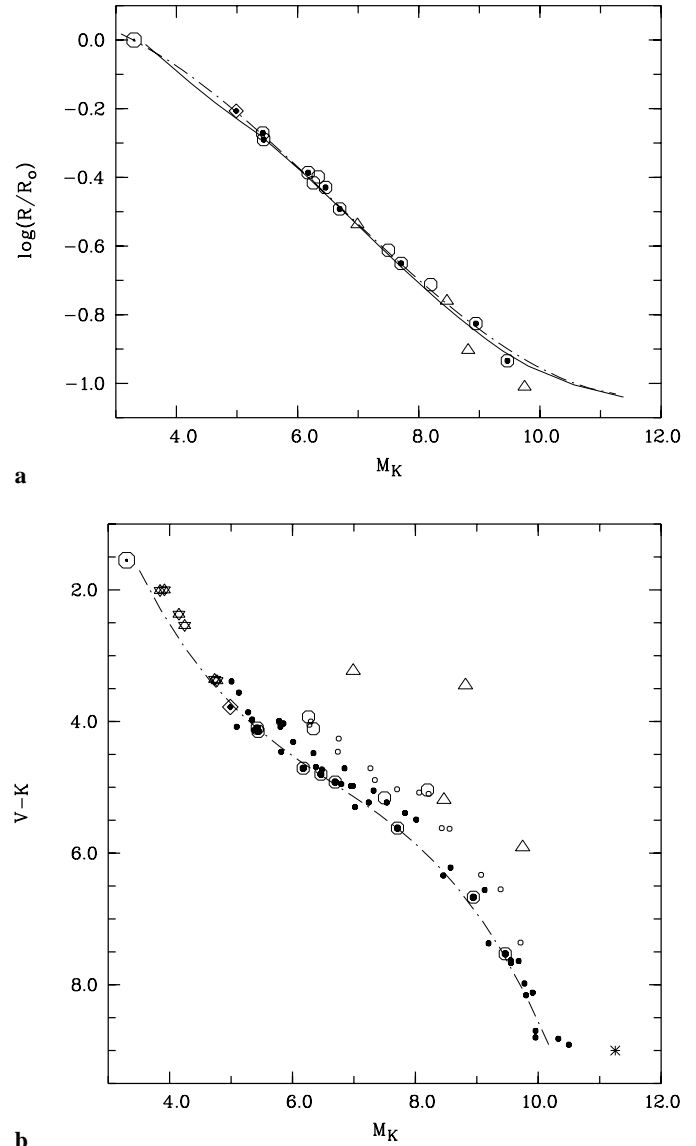


**Fig. 3.** **a** *Top panel:* Observationally determined radii of YY Gem and the L96 dwarfs (symbols as in Fig. 2) compared with the solar-metallicity ZAMS model radii of BCAH98 (solid curve). Also shown is the polynomial representation of the model curve by Eq. (7) (dot-dashed curve). **b** *Bottom panel:* Colour-magnitude diagram  $V - K$  vs.  $M_K$ . The stars from Henry & McCarthy (1993) are shown as small solid and open circles (see text), the stars from Reid & Gizis (1997) as stars and GD165B as an asterisk. The dot-dashed curve represents the location of ZAMS stars with near-solar metallicity according to Eq. (8).

60 single or presumed single YD/OD main-sequence stars. The colour-magnitude diagram of these stars is shown in Fig. 3b. Six K-stars are from Reid & Gizis (1997) (stars) and 53 M-stars from Henry & McCarthy (1993) (small solid and open circles). The L-star GD165B represents the transition to the brown-dwarf regime (asterisk).

**Table 2.** Radii of YD and OD dwarfs from L96. The columns indicate (1) the name, (2) the spectral type, (3) the kinematic population class, (4) the parallax in mas from L96, (5)  $V - K$ , (6)  $I_c - K$ , (7) the absolute K-magnitude, in case of binaries the mean of the two components, (8) the logarithm of the radius in units of  $R_\odot$  as derived observationally by L96, (9) the radius obtained from  $V - K$  in Column 5 with Eqs. (2) and (6) for the  $[M/H] \simeq 0$  stars and with  $S_K(V - K)$  in Table 1 for the  $[M/H] \simeq -0.5$  stars, (10) the radius derived from  $I_c - K$  in Column 5 with  $S_K(I_c - K)$  in Table 1 and Eqs. (2), (11) the radius from Eqs. (7), and (12) the radius given by Lacy (1977) corrected to the parallax in Column 3.

(1)	(2)	(3)	(4)	(5)	(6)	(7)	(8)	(9)	(10)	(11)	(12)
Name	$Sp$	Pop	$\pi$ mas	$V - K$	$I - K$	$M_K$	L96	log( $R/R_\odot$ ) from			
								$S_K(V - K)$	$S_K(I_c - K)$	$R(M_K)$	Lacy (1977)
<i>(1) Young disk M-dwarfs with <math>[M/H] \simeq 0</math></i>											
Gl65 $\overline{AB}$ <sup>1)</sup>	M6-	YD	373.8	6.67	2.95	8.94	$-0.83 \pm 0.03$	-0.85	-0.84	-0.84	-0.81
Gl195A	M2:	YD	76.4	4.10	1.97	5.43	$-0.27 \pm 0.03$	-0.28	-0.28	-0.28	
Gl206 $\overline{AB}$ <sup>1)</sup>	M3.5	YD	73.6	4.92	2.25	6.69	$-0.49 \pm 0.04$	-0.49	-0.48	-0.49	
Gl268 $\overline{AB}$ <sup>1)</sup>	M4.5	YD	165.1	5.62	2.57	7.71	$-0.65 \pm 0.01$	-0.66	-0.63	-0.65	-0.65
Gl388	M3	YD	205.5	4.71	2.20	6.17	$-0.39 \pm 0.02$	-0.40	-0.38	-0.40	-0.30
Gl494A <sup>2)</sup>	M1.5	YD	92.5	4.15	2.10	5.44	$-0.29 \pm 0.04$	-0.28	-0.26	-0.28	
Gl896A	M3.5	YD	150.1	4.80	2.20	6.46	$-0.43 \pm 0.03$	-0.45	-0.44	-0.45	
GJ1111	M6.5	YD	275.8	7.53	3.27	9.46	$-0.93 \pm 0.02$	-0.90	-0.92	-0.90	-0.97
<i>(2) Old disk M-dwarfs with <math>[M/H] \simeq -0.5</math></i>											
Gl213	M4	O/H	168.1	5.16	2.33	7.50	$-0.61 \pm 0.02$	-0.58	-0.59	-0.62	-0.51
Gl411	M2	OD	394.4	4.11	1.96	6.34	$-0.40 \pm 0.02$	-0.41	-0.43	-0.43	-0.33
Gl699	M4	O/H	546.0	5.04	2.26	8.20	$-0.71 \pm 0.03$	-0.72	-0.75	-0.73	-0.68
Gl908	M1	OD	174.6	3.93	1.90	6.26	$-0.42 \pm 0.02$	-0.41	-0.42	-0.41	-0.34

<sup>1)</sup>  $\overline{AB}$  refers to the mean of the two binary components.

<sup>2)</sup> Following L96, the contribution by the faint secondary is neglected.

We consider the calibrator stars first. In Table 2, we compare the L96 radii with those obtained from the Barnes-Evans type relations  $S_K(V - K)$  and  $S_K(I_c - K)$  and from  $M_K$ :

Column 9: Radii of YD or  $[M/H] \simeq 0$  stars derived from the observed  $V - K$  with Eqs. (2) and (6). Radii of OD stars obtained correspondingly, but with the theoretical  $S_K(V - K)$  relation for  $[M/H] = -0.5$  of Table 1 instead of Eq. (6).

Column 10: Radii obtained from the observed  $I_c - K$  with the theoretical  $S_K(I_c - K)$  relations of Table 1 for the  $[M/H] = 0$  or the  $[M/H] = -0.5$  stars.

Column 11: Radii derived from  $M_K$  with Eq. (7) without regard of metallicity, assuming the stars to be on the ZAMS.

The radii in Column 11 and the YD radii in Column 9 agree with the L96 radii within 5% or  $\Delta \log R = 0.02$  which reflects the goodness of the fits. The small differences between the radii in Columns 10 and 8, on the other hand, demonstrate the close agreement between theory and observation.

Application of the Barnes-Evans type relations to the complete sample of 60 K/M dwarfs requires at least a rough estimate of their metallicity. For this purpose, we divide the sample into a *brighter* and a *fainter* subsample, containing stars within  $\sim 1$  mag of the bright limit in  $M_K$  (small solid circles in Fig. 3b) and stars within  $\sim 1-2$  mag from the bright limit (small open circles), respectively. This subdivision can be interpreted in terms of different metallicity if age is not an influencing factor. Assuming all stars to be close to the ZAMS, the two subsamples correspond to stars of near-solar metallicity and a metallicity re-

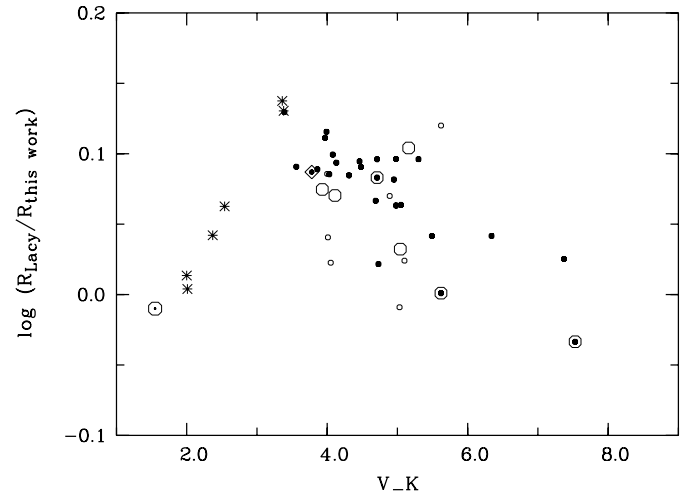


**Fig. 4.** Differences in  $\log(R/R_\odot)$  between the radii given by Lacy (1977) and here: (i) L96 YD/OD stars (Table 2, Column 8, large symbols as in Fig. 2) and (ii) stars in Table 3, radii derived from  $S_K(V - K)$  (Column 8, small symbols as in Fig. 3).

duced by  $\Delta[M/H] \simeq 0.5$ , respectively (e.g. L96). In deriving the radii, we proceed as above for the L96 stars. Table 3 provides the observed properties and the derived radii. The restriction to single stars is important in order to avoid the larger radii falsely assigned to unrecognized binaries.

Column 12 of Table 2 and Column 11 of Table 3 list the radii given by Lacy (1977) adjusted to the parallaxes used here.

**Table 3.** Radii of single or presumed single field M-dwarfs from the list of Henry & McCarthy (1993). The columns indicate (1) the name, (2) the spectral type, (3) the kinematic population class if available (4) the parallax, (5)  $V - K$ , (6)  $I_c - K$ , (7) the absolute K-magnitude, (8) the logarithm of the radius in units of  $R_\odot$  as derived from Eqs. (2) and (6), (9) same as derived from the theoretical  $S_K(I_c - K)$  relation of BCAF98 for  $[M/H] = 0$  in Fig. 2a, (10) same as derived from Eq. (7), and (11) the radius as given by Lacy (1977), adjusted to the parallax in Column 4.

(1)	(2)	(3)	(4)	(5)	(6)	(7)	(8)	(9)	(10)	(11)
Name	$Sp$	Pop	$\pi$ mas	$V - K$	$I_c - K$	$M_K$	$S_K(V - K)$	log ( $R/R_\odot$ ) from		Lacy (1977)
								$S_K(I_c - K)$	$R(M_K)$	
<i>(1) Brighter M-dwarfs, assumed to have <math>[M/H] \simeq 0</math></i>										
Gl68	K1		138.9	2.01	1.15	3.84	-0.07	-0.07	-0.06	-0.07
Gl105A	K3		125.6	2.37	1.30	4.15	-0.12	-0.12	-0.09	-0.07
Gl105B	M4-	O	138.7	5.05	2.26	7.32	-0.61	-0.60	-0.59	-0.54
Gl109	M3+	Y	125.6	4.69	2.24	6.38	-0.44	-0.42	-0.43	-0.37
Gl166A	K1	O	198.2	2.00	1.12	3.91	-0.09	-0.08	-0.07	-0.08
Gl166C	M4.5	O	198.2	5.23	2.36	7.53	-0.64	-0.63	-0.62	
Gl205	M1.5	O	175.5	4.08	2.01	5.09	-0.21	-0.21	-0.23	-0.11
Gl229	M1.5	Y	173.2	3.97	1.96	5.34	-0.27	-0.27	-0.26	-0.16
Gl251	M3	Y/O	173.7	4.73	2.23	6.48	-0.46	-0.44	-0.45	-0.43
Gl273	M3.5	O	263.3	4.98	2.28	6.98	-0.54	-0.53	-0.53	-0.45
Gl300	M4+	Y	170.0	5.39	2.49	7.83	-0.69	-0.67	-0.67	
Gl338A	M0	Y	162.0	3.56	1.82	5.13	-0.25	-0.26	-0.23	-0.16
Gl380	K7	Y/O	205.2	3.38	1.76	4.77	-0.19	-0.20	-0.18	-0.06
Gl393	M2	Y/O	136.2	4.31	2.07	6.01	-0.39	-0.38	-0.37	-0.30
Gl402	M4	Y/O	145.9	5.23	2.44	7.24	-0.58	-0.55	-0.58	
Gl406	M6	O	419.1	7.37	3.31	9.19	-0.86	-0.86	-0.87	-0.83
Gl408	M3	Y	144.6	4.48	2.09	6.34	-0.44	-0.44	-0.43	-0.35
Gl447	M4+	O	299.6	5.49	2.51	8.01	-0.72	-0.70	-0.70	-0.68
Gl450	M2	O	107.8	4.08	2.00	5.80	-0.36	-0.35	-0.34	
Gl514	M1	O	139.5	3.99	1.98	5.78	-0.36	-0.35	-0.33	-0.24
Gl555	M4	Y/O	159.0	5.30	2.44	7.02	-0.53	-0.51	-0.54	-0.44
Gl570A	K4		169.3	2.54	1.20	4.24	-0.13	-0.14	-0.11	-0.06
Gl581	M3.5	Y/O	158.2	4.71	2.20	6.85	-0.53	-0.52	-0.51	-0.44
Gl628	M3.5	Y	234.5	4.98	2.30	6.95	-0.54	-0.52	-0.53	-0.47
Gl644C	M7	O	154.0	7.98	3.42	9.78	-0.95	-0.96	-0.93	
Gl673	K7	O	129.5	3.36	1.75	4.73	-0.18	-0.19	-0.17	-0.04
Gl701	M2	O	126.6	4.03	1.97	5.85	-0.37	-0.37	-0.35	-0.28
Gl752A	M3	O	170.3	4.46	2.14	5.82	-0.34	-0.32	-0.34	-0.24
Gl752B	M8	O	170.3	8.70	4.00	9.96	-0.94	-0.93	-0.95	
Gl809	M1	O	134.2	3.86	1.87	5.28	-0.26	-0.28	-0.25	-0.17
Gl873	M3.5	Y/O	198.1	4.95	2.26	6.79	-0.51	-0.50	-0.50	-0.43
Gl880	M2	O	148.5	4.13	2.03	5.39	-0.27	-0.26	-0.27	-0.18
Gl884	M0-	O	128.1	3.39	1.75	5.01	-0.23	-0.25	-0.21	-0.10
Gl905	M5.5	O	316.8	6.34	2.89	8.45	-0.77	-0.75	-0.77	-0.72
GJ1156	M5	Y	101.5	6.22	2.76	8.57	-0.80	-0.78	-0.78	
GJ1245B	M5.5		220.2	6.56	2.83	9.16	-0.89	-0.89	-0.86	
LHS191	M6.5		59.2	7.63	3.26	9.55	-0.92	-0.93	-0.91	
LHS292	M6.5	O	220.9	7.64	3.24	9.68	-0.94	-0.96	-0.92	
LHS2065	M9		117.3	8.82	4.46	10.33	-1.01:	-0.95:	-0.98:	
LHS2397a	M8	O	68.7	8.80	4.18	9.95	-0.94	-0.91	-0.95	
LHS2471	M7	O	70.9	7.67	3.39	9.55	-0.92	-0.92	-0.91	
LHS2924	M9	O	92.4	8.91	4.54	10.50	-1.04:	-0.98:	-1.00:	
LHS2930	M7	Y/O	103.8	8.16	3.59	9.80	-0.94	-0.95	-0.94	
LHS3003	M7		157.0	8.12	3.60	9.91	-0.96	-0.97	-0.95	
GD165B	L		26.6		5.03	11.25		-1.02:	-1.03:	
<i>(2) Fainter M-dwarfs, assumed to have <math>[M/H] \simeq -0.5</math></i>										
Gl015A	M1.5	O	281.2	4.05	1.91	6.28	-0.40	-0.42	-0.41	-0.38
Gl015B	M4-	O	281.2	5.10	2.28	8.22	-0.72	-0.75	-0.73	-0.70
Gl054.1	M4.5	O	267.4	5.63	2.48	8.56	-0.76	-0.78	-0.78	
G3-33	M4.5	O	224.8	5.62	2.50	8.43	-0.73	-0.75	-0.76	-0.61

**Table 3.** (continued)

(1)	(2)	(3)	(4)	(5)	(6)	(7)	(8)	(9)	(10)	(11)
Name	$S_p$	Pop	$\pi$ mas	$V - K$	$I_c - K$	$M_K$		log( $R/R_\odot$ ) from		
							$S_K(V - K)$	$S_K(I_c - K)$	$R(M_K)$	Lacy (1977)
GI412A	M1	O	203.0	4.00	1.98	6.30	-0.41	-0.41	-0.42	-0.32
GI412B	M6	O	203.0	6.55	2.78	9.39	-0.87	-0.89	-0.89	
GI445	M3.5	O	191.5	4.89	2.25	7.34	-0.56	-0.58	-0.59	-0.49
GI526	M1.5	O	183.7	4.01	1.97	5.78	-0.31	-0.31	-0.33	-0.27
GI625	M2	Y	152.2	4.26	2.05	6.75	-0.48	-0.49	-0.49	
GI643	M4	O	155.7	5.03	2.30	7.70	-0.63	-0.64	-0.65	-0.63
GI725A	M3	Y/O	288.1	4.46	2.00	6.74	-0.47	-0.50	-0.49	
GI725B	M3.5	Y/O	288.1	4.71	2.16	7.27	-0.56	-0.58	-0.58	
GI729	M4-	Y/O	342.3	5.08	2.30	8.06	-0.69	-0.71	-0.71	-0.87
GJ1002	M5.5	O	212.8	6.33	2.73	9.07	-0.82	-0.84	-0.85	
LHS523	M6.5	O	91.7	7.36	3.10	9.71	-0.88	-0.89	-0.93	

Compared with Lacy's results, our radii are smaller by up to  $\sim 25\%$ . Fig. 4 shows that there is a systematic trend for the difference between Lacy's radii and those determined by L96 or, for the additional stars, from our Barnes-Evans type relations  $S_K(V - K)$ . Very similar pictures obtain for the radii derived from the Barnes-Evans type relation  $S_K(I_c - K)$  (Table 3, Column 9) or directly from  $M_K$  (Table 3, Column 10, both not shown). The deviation of Lacy's from our radii assumes a maximum at spectral type K7 and vanishes for early K and for late M dwarfs. Much of this is due to the different surface brightness calibrations for giants (used by Lacy) and dwarfs (used here) which reach a maximum separation at  $V - I_c \simeq 1.6$ ,  $V - K \simeq 3.4$ , or spectral class K7 (Fig. 1). The remainder is due to differences in the individual giant relations used by Lacy (Barnes & Evans 1976) and by us (Eq. [3] and Dumm & Schild 1997). Lacy discussed a deviation of similar magnitude and colour-dependence between the surface brightness of giants and the theoretical ZAMS dwarf models of Copeland et al. (1970). He interpreted it as being entirely due to inadequacies of the models. We now know that (i) the surface brightness of mid-K to mid-M dwarfs is, in fact, higher than that of giants of the same colour and (ii) the recent dwarf models (BCAH98) predict somewhat larger radii than the early models which reduces the discrepancy noted by Lacy (1977).

Finally, we discuss the systematic errors in our radius calibration which is tied to the observational results of L96 and to the theoretical predictions of BCAH98. Our radius scale for stars of near-solar metallicity is based on the results of L96 which may still be in error by some  $\sim 6\%$  or 0.03 in log  $R$  (radii too small, see Sect. 2). The difference of this radius scale to the BCAH [M/H] = 0 model is  $\sim 2\%$ . Clemens et al. (1998), on the other hand, quote radii for stars later than M2 at given mass which are larger than those predicted by BCAH98 by  $\sim 20\%$ . Part of this discrepancy may be due to remaining uncertainties in the bolometric corrections (Sect. 2) and part to the transformations used by them. Clemens et al. adopt the  $M_{\text{bol}}$  scale and the temperature scale of L96 to deduce radii which are higher by  $\sim 7\%$  than those quoted by L96. They employ the *mean observational*  $M_V(M)$  relation of Henry & McCarthy (1993)

in order to convert absolute visual magnitudes  $M_V$  to masses  $M$ . For  $M < 0.2 M_\odot$ , this relation presently relies on 10 stars only (Henry et al. 1999). It shows substantial scatter which may be caused by a spread in ages and metallicity and/or still by the inclusion of erroneous masses. The masses of the YD binary Wolf 424 ( $0.143 \pm 0.011$  and  $0.131 \pm 0.010 M_\odot$ ) were recently re-determined with the *HST* Fine Guidance Sensors (Torres et al. 1999) and agree perfectly with the predictions of BCAH98. We expect that a better definition of the mass-radius relation will become available soon (Henry et al. 1999) and allow the remaining discrepancies to be resolved.

## 6. Conclusions

We conclude that the effects of gravity on the visual surface brightness of M-giants and M-dwarfs as well as the effects of metallicity on the surface brightness of M-dwarfs are discernible in the data and agree quantitatively with the predictions of recent stellar models (Alibert et al. 1999, Hauschildt et al. in preparation, BCAH98). The surface brightness values of giants and dwarfs agree for spectral types earlier than  $\sim K2$  and later than  $\sim M5$  and reach a maximum separation at spectral type K7. Although small, this difference must be taken into account when estimating dwarf radii by the surface brightness method.

We present improved Barnes-Evans type relations which allow to determine the radii of late-type giants and dwarfs of known distances with a remaining systematic uncertainty of  $\sim 6\%$ . Our calibration is based on the M-dwarf radii determined by L96 from fits of the *NextGen* model atmospheres of Hauschildt et al. (1999) to the observed spectra of these stars. While these radii are not purely observational, the internal consistency of atmosphere calculations, stellar models, and observation has reached a high degree of excellency. We conclude that the differences between observed and predicted surface brightness for stars on the lower main sequence have largely been resolved.

*Acknowledgements.* We thank Mel Dyck for sending us his photometry of giants and Boris Gänsicke, Frederick Hessman, and Klaus Reinsch for many discussions and the referee H. Schild for helpful comments.

This research has made use of the on-line version of the HIPPARCOS catalogue. IB thanks the Universitäts-Sternwarte, Göttingen, for hospitality and the APAPE (PROCOPE contract 97151) for travel support. The work of PH was supported in part by NASA ATP grant NAG 5-3018, LTSA grant NAG 5-3619 and NSF grant AST-9720804 to the University of Georgia. Some of the calculations presented in this paper were performed on the IBM SP2 and SGI Origin 2000 of the UGA UCNS, at the San Diego Supercomputer Center (SDSC) and at the National Center for Supercomputing Applications (NCSA), with support from the National Science Foundation, and at the NERSC with support from the DoE. We thank all these institutions for a generous allocation of computer time.

## References

- Alibert Y., Baraffe I., Hauschildt P.H., Allard F., 1999, A&A 344, 551  
 Baraffe I., Chabrier G., Allard F., Hauschildt P.H., 1998, A&A 337, 403 (BCAH98)  
 Barnes T.G., Evans D.S., 1976, MNRAS 174, 489  
 Barnes T.G., Dominy J.F., Evans D.S., et al., 1977, MNRAS  
 Bailey J., 1981, MNRAS 197, 31  
 Beuermann K., Baraffe I., Kolb U., Weichhold M., 1998, A&A 339, 518 (Paper I)  
 Clemens J.C., Reid I.N., Gizis J.E., O'Brien M.S., 1998, ApJ 496, 352  
 Copeland H., Jensen J.O., Jørgensen H.E., 1970, A&A 5, 12  
 Diamond C.J., Jewell S.J., Ponman T.J., 1995, MNRAS 274, 589  
 Dumm T., Schild H., 1998, New Astr. 3, 137  
 Dyck H.M., van Belle G.T., Thomson R.R., 1998, AJ 116, 981  
 Fouqué P., Gieren W.P., 1997, A&A 320, 799  
 Hauschildt P.H., Allard F., Baron E., 1999, ApJ 512, 377  
 Henry T.J., McCarthy W. Jr., 1993, AJ 106, 773  
 Henry T.J., Franz O.G., Wasserman L.H., et al., 1999, ApJ 512, 864  
 Lacy C.L., 1977, ApJS 34, 479  
 Leggett S.K., Allard F., Berriman G., Dahn C.C., Hauschildt P.H., 1996, ApJS 104, 117 (L96)  
 Leung K.-C., Schneider D.P., 1978, AJ 83, 618  
 Reid I.N., Gizis J.E., 1997, AJ 113, 2246  
 Schlegel D.R., Finkbeiner D.P., Davis M., 1998, ApJ 500, 525  
 Tinney C.G., Mould J.R., Reid I.N., 1993, AJ 105, 1045  
 Thomas H.-C., Beuermann K., 1998, In: Breitschwerdt D., et al. (eds.) The Local Bubble and Beyond. Springer Lect. Not. Phys. 506, 247  
 Torres G., Henry T.J., Franz O.G., Wasserman L.H., 1999, AJ 117, 562